Direct Visualization of Live Zebrafish Glycan via Single-step Metabolic Labeling with Fluorophore-tagged Nucleotide Sugars

Senlian Hong[§,#], Pankaj Sahai-Hernandez[†,#], David Traver[†,*] and Peng Wu[§,*].

[§]Department of Molecular Medicine, The Scripps Research Institute, La Jolla, California, 92037, U.S.A. [†]Department of Cellular and Molecular Medicine, University of California at San Diego, La Jolla, California, U.S.A. [#]These authors contributed equally to this work.

ABSTRACT: Dynamic turnover of cell-surface glycans is involved in a myriad of biological events, making this process an attractive target for in vivo molecular imaging. The metabolic glycan labeling coupled with 'bioorthogonal chemistry' has paved the way for visulizing glycans in living organisms. However, a two-step labeling sequence is required, which is prone to tissue penetration difficulties of the imaging probes. Here, by exploring the substrate promiscuity of endogenous glycosyltransferases, we developed a single-step fluorescent glycan labeling strategy by using fluorophore-tagged analogs of nucleotide sugars directly. Injecting the fluorophore-tagged sialic acid and fucose into the yolk of zebrafish embryos at the one-cell stage enables a systematic imaging of sialylation and fucosylation in live zebrafish embryos at various developmental stages. From these studies, we obtained insights into the role of sialylated and fucosylated glycans in zebrafish hematopoiesis.

Metabolic oligosaccharide engineering (MOE) coupled with the bioorthogonal chemical reporter strategy has opened an avenue for labeling and visualizing glycans in living organisms.[1-5] In this approach, the cell's glycan biosynthetic machinery is exploited to install a biorthogonal chemical group onto cell surface glycans, which is then covalently labeled in a second step with a complementary probe.[6] However, this strategy has a few intrinsic limitations, such as the biocompatibility of a chosen bioorthogonal reaction and poor deep-tissue penetration of probes.[7]

Chemoenzymatic glycan editing, however, may enable the direct incorporation of a fluorescently labeled monosaccharide directly without the requirement of a second-step covalent reaction. By using recombinant sialytransferases (STs) and fucosyltransferases (FTs) with broad donor substrate scopes, sialic acid (Sia) and fucose (Fuc) conjugated with fluorescent dyes can be transferred directly to the cell surface from the corresponding nucleotide sugars.[8-11] Inspired by these findings by us and other, as well as the recent findings that fluorescently labeled trehalose and *N*-acetylglucosamine can be directly incorporated into the cell wall of *M. tuberculosis*[12] and intracellular *O*-Glc*N*Acylated proteins in cultured mammalian cells[13], respectively, we sought to explore the feasibility of directly incorporating fluorophore-labeled monosaccharides into cellular glycans in living organisms by exploiting the substrate promiscuity of endogenous glycosyltransferases (Fig. 1a).

We evaluated this design in the live zebrafish embryo due to it optical transparency, external fertilization and amenability to genetic and embryological manipulations.[14-16] First, we synthesized a fluorophore-labeled CMP-N-acetylneuraminic acid (CMP-Neu5NAc) and microinjected it into the yolk sack of the embryo at the one-cell stage[17], which enables the injected nucleotide sugar to disperse and incorporate into all daughter cells.

It is known that many sialyltransferases (STs) tolerate large substituents at C9 of Neu5NAc.[14,15] Therefore, we synthesized CMP-Sia-*sulfo*-Cy5 (probe A) by coupling CMP-9AzSia[16] with Al-*sulfo*-Cy5 via the ligand (BTTP) assisted copper-catalyzed azide-alkyl [3+2] cycloaddition (CuAAC)[17]. Probe A was injected into the yolk of

one-cell stage zebrafish embryos (Fig. 2a).[18] The treated embryos were then subjected to fluorescent imaging at various developmental stages. As shown in the supplimentary Fig. s1, overwhelming fluorescent signals in the yolk due to the accumulation of probe A prevented the visualization of the incorporated sialic acid in other tissue structures during the early embryogenesis. To our delight, the incorporation of probe A in several dinstinct tissue structures became apparent between 14 hours' post fertilization (hpf), and 28 hpf (Fig. s1).

To confirm that probe A was metabolically incorporated into glycoproteins, the lysates of the deyolked embryos were analyzed using an in-gel fluorescence assay. We detected strong A-dependent Cy5 signals in SDS-PAGE resolved proteins with molecular weight ranging from 30-250 kD, strongly suggeting that CMP-Sia-*sulfo*-Cy5 was metabolically incorporated onto sialylated glycoproteins (Fig. 2b).

We then performed a systematical imaging of sialylation using probe A. At 24 hpf, we observed intensive Cy5 fluorescence in the head and trunk regions (Fig. 2c, movie s1 and s2). The eye and hindbrain areas of the head, the somatic tissue, muscle cells and introhypochord of the trunk exhibited strong Cy5 fluorescence in particular. In the control embryos that injected with CMP-9AzSia and Al-*sulfo*-Cy3, only negligible background Cy5 signals were detected (Fig. 2d). These observations were consistent with what was reported by Bertozzi and corworkers, in which BCNSia was used as the metabolic substrate and the detection was realized by reacting with a fluorogenic tetrazine probe injected into the caudal vein. Via their approach, imaging can only be lauched at 30 hpf, which is the earliest time that the caudal vein starts to form. Since the incorporation of unnatural analogs onto glycan could potentially interfere their biological functions, we further analyzed the morphological defects of zebrafish embryo injected with different concentrations of probe A (2.5, 5 or 10 pmol). At 24 hpf (Fig. s2) we did not observe apparent toxicity in the probe-injected group compared to the non-injected ones.

Then, we expanded this design for the directly probing another type of glycosylation (i.e. fucosylation). We prepared a Cy3-tagged GDP-Fuc analog by conjugating the GDP-FucAz[19] (or *in situ* generated GDP-FucAz) with Al-*sulfo*-Cy3 (Fig. s3a). The

embryos treated GDP-FucAz-s*ulfo*-Cy3 (probe B) exhibited gross morphological defects (twisted notochord *et al*), and the defects became more severe when the injected dose of probe B was increased (Fig. s4). The same phenotype was also observed in the GDP-FucAz injected group, and the embryos injected with a mixture of GDP-FucAz and Al-*sulfo*-Cy3. As an alternative, we chose to use GDP-6-alkylfucose (GDP-FucAl) with better biocompatiblility to prepare the Cy3-tagged analog (GDP-Fuc-*sulfo*-Cy3, Fig. s3b).[20] To our delight, embryos treated with GDP-Fuc-*sulfo*-Cy3 (probe C) exhibited no aparrent defects compared to the natural GDP-Fuc treated group.

To image fucosylated glycan in live zebrafish, we injected the *sulfo*-Cy3-bearing probe B and probe C into the yolk, and performed confocal imaging of the treated embryos at 24 hpf (movie s3 and s4). Embryos injected with both probes showed intensive Cy3 fluorescence in the brain and trunk regions without observable differences in labeling patterns, while in control groups embryos showed no specific labeling except for the dye trapped within the yolk. Due to the toxicity of probe B, a systematically imaging of fucosylation was conducted with probe C, even though probe C shown weaker incorporation. Confocal images of live zebrafish embryos injected with probe C revealed a highly-localized distribution of labled fucosides in the head (lateral, ventral and dorsal views) and trunk (lateral view) (Fig. 3, movie s5 and s6). Aboundant fucosylation was also detected in the eye, olfactory placode, midbrain, hindbrain, hypochord, dorsal fin, blood vessel and the caudal hematopoietic tissue (cht). The incorporation was more intense in neural structures such as the midbrain and the hindbrain. Interestingly, the midbrain-hindbrain boundary (mhb) does not show any incorporation of the unnatural fucose. Moreover, this strategy also enabled a time-lapse tracking of fucosylated glycans in live zebrafish embryos. For example, Cy3-labeled fucoside were found to be aboundantly expressed in the retina and the optical cup of eyes, and dynamicly moving along the ganglion cells of acetylated microtubules (Fig. 3 p2’-t1 and p2’-t2, movie s7).

The ability to simutaneously visualize distinct biomolecues in vivo is of essential importance for understanding normal and diseased processes. We then evaluated the feasibility to visualize sialylated and fucosylated glycans in parallel. To this end, we

co-injected probe 1 and probe 3 at 1:1 molar ratio into the yolk of zebrafish embryos and conducted imaging at 24hpf. As the colocalization shown in Fig. 4a, sialylated glycans have broader distributions than fucosylated counterparts. The blood vessel is the region showing the strongest co-localization of both glycans. However, these two types of glycans also exhibit many distinct distribution patterns. For example, sialylation was aboundantly detected in the notochord, muscular cell types, while fucoysaltion was more localzied in the vascular endothelial region.

Next, we directly compared the labeling patterns of the single-step glycan lableing to the two-step bioorthogonal chemical reporter strategy. We co-injected probe 3 and GDP-FucAz into the same embryo, and the metabolically incorporated FucAz were fluorescently labeled with Al-*sulfo*-Cy5 by BTTPS-assisted CuAAC reaction at 24 hpf. In deep tissues such as the cht region, we only observed Cy3 signal, but not that of Cy5. Likewise, only very weak Cy5 signal was deteatable in the trunk and the brain, which is likely due to the poor permeability of labeling reagents into the deep-tissue of live zebrafish embryos. The observation that much stronger Cy5 signal was detected at the tip of the tail compared to the Cy3 signal is likely caused by the same issue (Fig. s5).

To exclude the possibility that the observed labeling patterns were generated by the unincorporated probes circling in the blood or diffusing into the tissue matrix, a hematopoietic mutant line known as 'Cloch' [21] was used to repeat our labeling experiments. In this mutant (cloche-/-) no blood circling system including cht is formed due to the developmental defects of blood and endothelial cells. In these mutant embryos injected with probe A or C, robust probe-dependent fluorescence was still detected in the trunk and the head regions. Likewise, similar labeling patterns were observed in the treated, wildtype like embryos (cloche+/-) that have developing cht. However, in these embryos the loss of the labeling in the cht region was detected (Fig. 4b, c, movie s8-s11). Based on these observations, we reasoned that the background fluorescence generated by the free, unincorporated probes in the blood stream is negligible.

The Caudal Hematopoietic Tissue (cht), a transient vascular plexus formed by the ramification of the caudal vein, provides the niche microenvironment for supporting the

development of hematopoietic stem cells (HSCs).[22] The cht is of vital importance for the maturation of blood cells and immune cells. To explore possible biological functions of glycans in this compartment, we imaged the probe A or probe C-treated transgenic line Tg(cMyb:eGFP)[23] whose HSCs produced in the definitive hematopoiesis can be tracked by eGFP expression (Fig. 4d, movie s12 and s13). Definitive hematopoiesis produces multipotent blood cells that give rise to multiple different lineages through cellular intermediates and support blood cell development throughout the life of the zebrafish. In the cht region, we observed that the fluorescently labeled sialosides and fucoside were present in cells that are in direct contact with the eGFP-expressing HSCs, but not in HSC themselves. As many studies reported that sialyl-Lewis X (sLe^X, Siaα2-3Galβ1-4(Fucα1-3)-GlcNAc) plays critical roles in mediating leukocytes adhesion and lymphocytes homing,[24,25] we further immuostained sLe^X epitopes in Tg(cMyb:eGFP) embryos with an anti-CLA antibody (Fig. 4d). Despict the high fluorescence background, the intensive staining of the cht region was mainly found in the extracellular matrix, rather than co-localizing with HSCs. This observation strongly suggested that interactions mediated by sialylated and fucosylated glycans such as sLe^X are involved in the HSC development and biology.

In conclusion, we demonstrated that fluorophore-tagged CMP-sialaic acid and GDP-fucose (probe A-C) injected into the yolk of zebrafish embryos were incorporated onto cellular glycoconjugates, enabling the direct deep-tissue visualization of sialylated and fucosylated glycans. Using this approach, time lapse, high-resolution, and sensitive confocal imaging of these biologically important glycans in zebrafish embryogenesis was realized. We are now extending this design for one-step incorporation of affinity tags into target glycans for glycoproteomics analysis. The elucidation of biological functions of these glycan epitopes in zebrafish hematopoiesis is currently under investigation.

Supporting Information

Additional figures, movies, materials and methods

REFERENCES

1. Laughlin, S. T., Baskin, J. M., Amacher, S. L. & Bertozzi, C. R. In vivo imaging of membrane-associated glycans in developing zebrafish. *Science* **320,** 664–667 (2008).
2. Laughlin, S. T. & Bertozzi, C. R. Imaging the glycome. *Proc. Natl. Acad. Sci. U.S.A.* **106,** 12–17 (2009).
3. Laughlin, S. T. & Bertozzi, C. R. In vivo imaging of Caenorhabditis elegans glycans. *ACS Chem. Biol.* **4,** 1068–1072 (2009).
4. Xie, R. *et al*. Targeted imaging and proteomic analysis of tumor-associated glycans in living animals. *Angew. Chem. Int. Ed. Engl.* **53,** 14082–14086 (2014).
5. Kang, K. *et al.* Tissue-based metabolic labeling of polysialic acids in living primary hippocampal neurons. *Proc. Natl. Acad. Sci. U.S.A.* **112,** E241–8 (2015).
6. Prescher, J. A. & Bertozzi, C. R. Chemistry in living systems. *Nat. Chem. Biol.* **1,** 13–21 (2005).
7. Bertozzi, C. R. A decade of bioorthogonal chemistry. *Acc. Chem. Res.* **44,** 651–653 (2011).
8. Capicciotti, C. J. *et al.* Cell-Surface Glyco-Engineering by Exogenous Enzymatic Transfer Using a Bifunctional CMP-Neu5Ac Derivative. *J. Am. Chem. Soc.* **139,** 13342–13348 (2017).
9. Sun, T. *et al.* One-Step Selective Exoenzymatic Labeling (SEEL) Strategy for the Biotinylation and Identification of Glycoproteins of Living Cells. *J. Am. Chem. Soc*. **138,** 11575–11582 (2016).
10. Hong, S. *et al.* Bacterial Glycosyltransferase-mediated Cell-surface Chemoenzymatic Glycan Editing: Methods and Applications. *bioRxiv* 322461 (2018). doi:10.1101/322461
11. Li, J. *et al.* A Single-Step Chemoenzymatic Reaction for the Construction of Antibody-Cell Conjugates. *ACS Cent Sci* **4,** 1633–1641 (2018).
12. Backus, K. M. *et al.* Uptake of unnatural trehalose analogs as a reporter for Mycobacterium tuberculosis. *Nat. Chem. Biol*. **7,** 228–235 (2011).

13. Tan, H. Y. *et al.* Direct One-Step Fluorescent Labeling of O-GlcNAc-Modified Proteins in Live Cells Using Metabolic Intermediates. *J. Am. Chem. Soc.* **140,** 15300–15308 (2018).
14. Ramya, T. N. C. *et al.* In situ trans ligands of CD22 identified by glycan-protein photocross-linking-enabled proteomics. *Mol. Cell Proteomics* **9,** 1339–1351 (2010).
15. Agarwal, P., Beahm, B. J., Shieh, P. & Bertozzi, C. R. Systemic Fluorescence Imaging of Zebrafish Glycans with Bioorthogonal Chemistry. *Angew. Chem. Int. Ed. Engl.* **54,** 11504–11510 (2015).
16. Han, S., Collins, B. E., Bengtson, P. & Paulson, J. C. Homomultimeric complexes of CD22 in B cells revealed by protein-glycan cross-linking. *Nat. Chem. Biol.* **1,** 93–97 (2005).
17. Wang, W. *et al.* Sulfated ligands for the copper(I)-catalyzed azide-alkyne cycloaddition. *Chem Asian J* **6,** 2796–2802 (2011).
18. Kimmel, C. B. & Law, R. D. Cell lineage of zebrafish blastomeres. I. Cleavage pattern and cytoplasmic bridges between cells. *Developmental Biology* **108,** 78–85 (1985).
19. Dehnert, K. W. *et al.* Metabolic labeling of fucosylated glycans in developing zebrafish. *ACS Chem. Biol.* **6,** 547–552 (2011).
20. del Amo, D. S. *et al.* Biocompatible Copper(I) Catalysts for in Vivo Imaging of Glycans. *J. Am. Chem. Soc.* **132,** 16893–16899 (2010).
21. Reischauer, S. *et al.* Cloche is a bHLH-PAS transcription factor that drives haemato-vascular specification. *Nature* **535,** 294–298 (2016).
22. Gore, A. V., Pillay, L. M., Venero Galanternik, M. & Weinstein, B. M. The zebrafish: A fintastic model for hematopoietic development and disease. *Wiley Interdiscip Rev Dev Biol* **7,** e312 (2018).
23. Bertrand, J. Y. *et al.* Haematopoietic stem cells derive directly from aortic endothelium during development. *Nature* **464,** 108–111 (2010).

24. Foxall, C. *et al.* The three members of the selectin receptor family recognize a common carbohydrate epitope, the sialyl Lewis(x) oligosaccharide. *J. Cell Biol.* **117,** 895–902 (1992).

25. Springer, T. A. Traffic signals for lymphocyte recirculation and leukocyte emigration: the multistep paradigm. *Cell* **76,** 301–314 (1994).

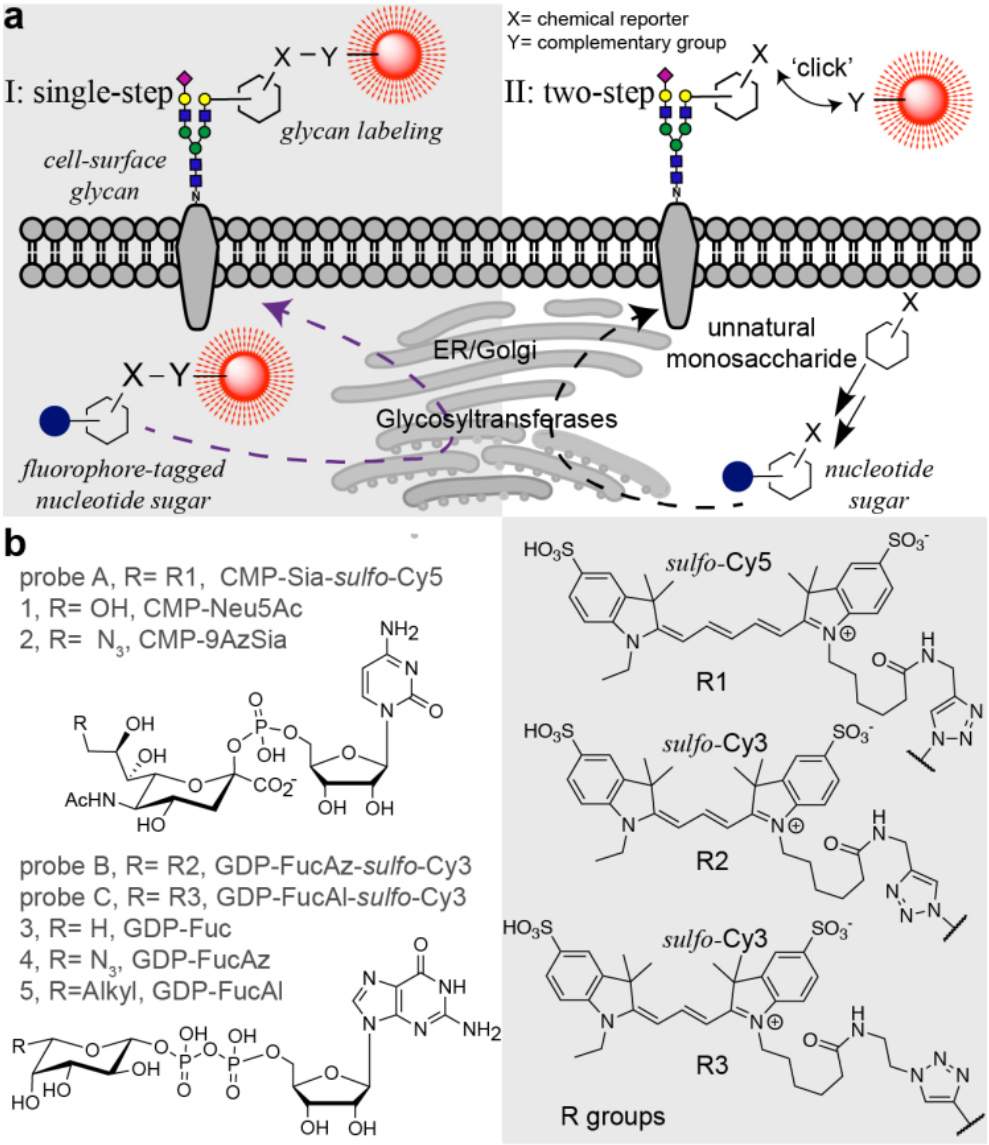

Figure 1. a), The single-step fluorescent glycan visualization via metabolic incorporation of unnatural fluorophore-tagged nucleotide sugars versus the conventional, two-step approach. b), Nucleotide sugar analogs functionalized with a chemical reporter (alkyl or azide) or a fluorophore (Cy3 and Cy5) used in this study.

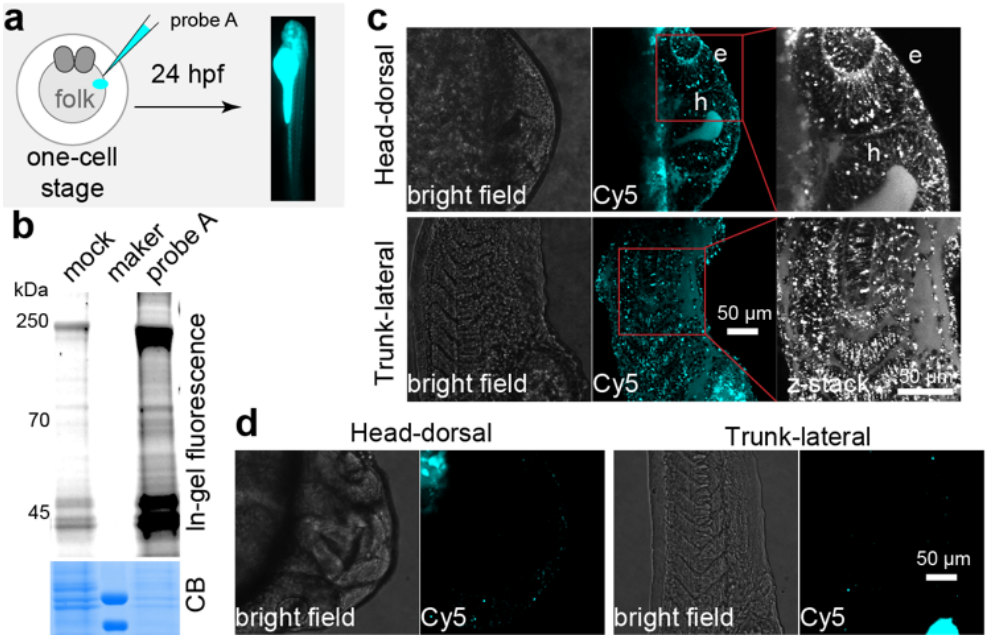

Figure 2. Metabolic incorporation of CMP-Sia-*sulfo*-Cy5 (probe A) onto sialylated glycan in live zebrafish embryos. a), Workflow of using probe A to fluorescently label sialylated glycan in zebrafish embryos. After a 24-hour incubation, the labeled glycoconjugates in live embryos was directly imaged. b), In-gel analysis of Cy5 fluorescence of labeled glycoproteins. The same counts of embryos were collected, deyolked, and the resulted lysis was loaded onto SDS-PAGE. The loading was evaluated by coomassie blue staining (CB). c, d), The confocal images of embryos injected with probe A (c), or prequenchaed reaction mixture (d, mock control). Intensive Cy5 fluorescence was detected in the eye (e) and hindbrain (h) regions of head, in the somatic tissue, muscle cells, and intro-hypochord of trunk.

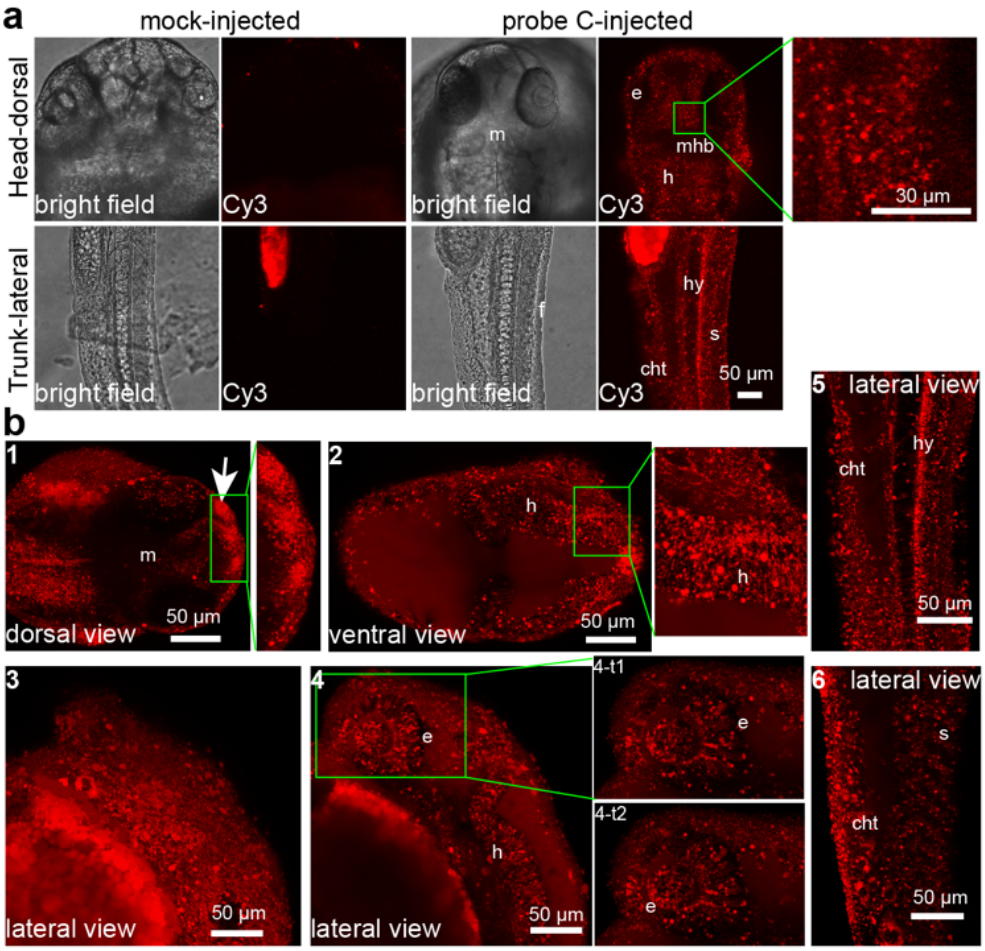

Figure 3. Systematic visualization of fucosylation in live zebrafish by metabolic incorporation of GDP-FucAl-*sulfo*-Cy3 (probe C) onto fucosylated glycans. a), confocal images of embryos injected with probe C or prequenchaed reaction mixture (mock control). In probe C-injected embryos, strong Cy3 fluorescence was detected in the eye (e), midbrain (m) and hindbrain (h) regions, while only negligible background fluorescence was detected in the midbrain-hindbrain boundary (mhb) as shown in the high magnification of the midbrain inset of head-dorsal view. b), Dorsal view (1 and 2) of a head in different depth, the developing mouth shown intensive fucosylation (arrow). Lateral views of head surface (3) and in deep-tissue (4). Lateral views of the tail (5 and 6). The robust incorporation of Cy3 was detected in somatic tissue (s), hypochord (h), dorsal fin (f), and in the vascular network of the caudal hematopoietic tissue (cht).

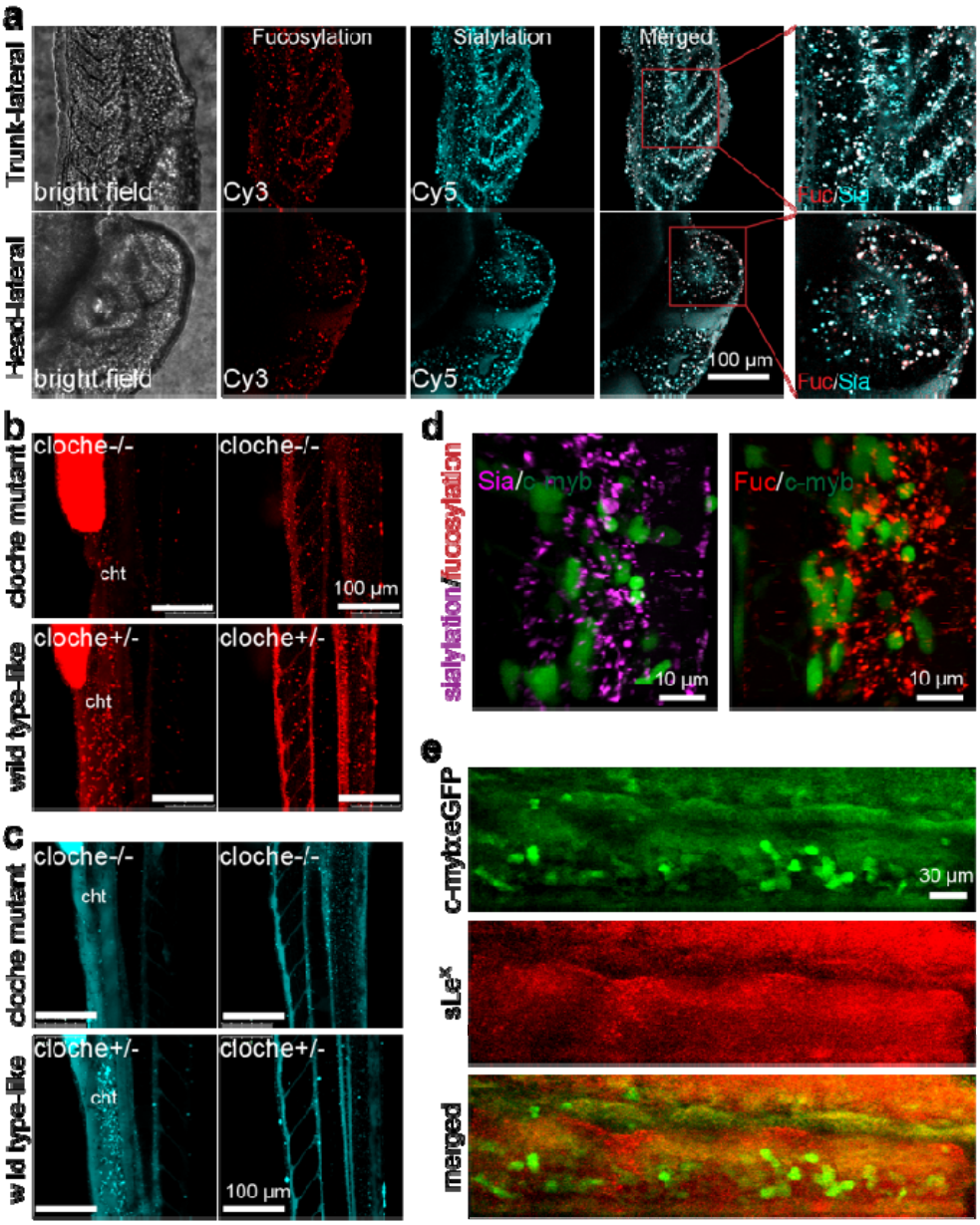

Figure 4. Simultaneous visualization of the deep-tissue fucosylation (Cy3 in red channel) and sialylation (Cy5 in cyan channel). a), The lateral view of zebrafish embryos co-injected with probe A and probe C. b, c), The trunk (lateral view) of cloche mutant (cloche-/-) or wild type-like line (cloche+/-) visualized at different depth. d), In the cht region of Tg(c-Myb:eGFP) embryos, HSCs (green channel) do not co-localize with the labeled of fucosides and sialosides. e), In Tg(c-Myb:eGFP) embryos HSCs do not co-localize with cells expressing sLe^X (red) in the cht region.